

**STATE KEY LABORATORY OF GEOLOGICAL
PROCESSES AND MINERAL RESOURCES**



地质过程与矿产资源 国家重点实验室

2005年论文成果汇编(上)



中国地质大学

前 言

地质过程与矿产资源国家重点实验室依托 4 个国家重点学科,整合教育部和国土资源部所属 6 个部级重点实验室的相关优质资源于 2002 年组建而成。2005 年,科技部正式批准实验室为国家重点实验室,同年参加全国地学领域国家及部门重点实验室评估中,获良好类重点实验室。

一年来,实验室根据《国家重点实验室建设管理办法》按照“联合、流动、开放、竞争”的方针,以矿产资源为核心,不断整合、优化内部资源,凝练学科方向,发挥中国地质大学地球科学多学科交叉、雄厚的研究基础、源源不断的人才资源、开放流动的科研环境、宽松自由的学术氛围、先进的实验仪器设备等方面的优势,紧紧围绕国家战略目标和地学前沿,通过基础与应用基础综合深入研究,为国家矿产资源战略部署和规划、区域矿产资源潜力评价、大型-超大型矿床发现,保障战略矿产资源持续供应,提供了有力的理论依据、技术支撑和科学咨询,继续保持了实验室在相关领域的国际先进地位,旨在建设成为国家组织高水平基础研究和应用基础研究,聚集和培养优秀科学家,开展学术交流的重要基地。

本论文集由吴春明、王丽娟经过反复整理编辑而成,是地质过程与矿产资源国家重点实验室科研人员近一年的科研成果汇编(论文 146 篇,其中 SCI 检索论文 37 篇、EI 检索论文 16 篇、ISTP 检索论文 21 篇;专著 6 部,其中主编 3 部、编写部分章节 3 部)。由于时间仓促、资料收集不够充分,其中必然有许多缺漏与不妥之处,请给予批评指正。这里对给予此论文集编写提供指导、帮助的领导、同事表示感谢!衷心地希望各位研究人员不断开拓创新,扎扎实实的做好科研工作,取得更多的科研成果。

2006 年 5 月

目 录

◆第一部分 SCI 检索论文◆

1. Shucheng Xie, Richard D. Pancost, 殷鸿福, 王红梅, Richard P. Evershed. Two episodes of microbial change coupled with permo/Triassic faunal mass extinction. **NATURE**, 2005, 434, 494-497. ----- (1)
2. Zhaochu Hu, Shan Gao, Shenghong Hu, Honglin Yuan, Xiaoming Liu and Yongsheng Liu. Suppression of interferences for direct determination of arsenic in geological samples by inductively coupled plasma mass spectrometry. **JAAS**, 2005, 20, 1263-1269. ----- (5)
3. JIANPING ZHENG, MIN SUN MEI FU ZHOU and PAUL ROBINSON. Trace elemental and PGE geochemical constraints of Mesozoic and Cenozoic peridotitic xenoliths on lithospheric evolution of the North China Craton. **Geochimica et Cosmochimica Acta**, 2005, 69(13), 3401-3418. ----- (12)
4. Yongsheng Liu, Shan Gao, Cin-Ty Aeolus Lee, Shenghong Hu, Xiaoming Liu, Honglin Yuan. Melt-peridotite interactions: Links between garnet pyroxenite and high-Mg# signature of continental crust. **Earth and Planetary Science Letters**, 2005, 234, 39-57. ----- (30)
5. J.P. Zheng, R.Y. Zhang, W.L. Griffin, J.G. Liou, S.Y. O'Reilly. Heterogeneous and metasomatized mantle recorded by trace elements in minerals of Donghai garnet peridotites, Sulu UHP terrane, China. **Chemical Geology**, 2005, 221, 243-259. ----- (49)
6. Deng Jun, Yang Liqiang, Sun Zhongshi, Wang Jianping, Wang Qingfei, Cheng Xueming and Zhou Yinghua. Late Paleozoic Fluid Systems and Their Ore-forming Effects in the Yuebei Basin, Northern Guangdong, China. **ACTA GEOLOGICA SINICA**, 2005, 79(5), 673-815. ----- (66)
7. Di Yongjun, Wu Ganguo, Zhang Da, Song Biao, Zang Wenshuan, Zhang Zhongyi and Li Jinwen. SHRIMP U-Pb Zircon Geochronology of the Xiaotongguanshan and Shatanjiao Intrusions and Its Petrological Implications in the Tongling Area, Anhui. **ACTA GEOLOGICA SINICA**, 2005, 79(6), 795-802. ----- (81)
8. Dong Guochen, Mo Xuanxue, Zhao Zhidan, Guo Tieying, Wang Liangliang and Chen Tao. Geochronologic Constraints on the Magmatic Underplating of the Gangdise Belt in the India-Eurasia Collision: Evidence of SHRIMP II Zircon U-Pb Dating. **ACTA GEOLOGICA SINICA**, 2005, 79(6), 787-794. ----- (89)
9. XIE Guiqing, MAO Jingwen, HU Ruizhong, LI Ruiling, JIANG Guohao, CAO Jinjian and ZHAO Junhong. Jurassic Intra-plate Basaltic Magmatism in Southeast China: Evidence from Geological and Geochemical Characteristics of the Chebu Gabbroite in Southern Jiangxi Province. **ACTA GEOLOGICA SINICA**, 2005, 79(5), 662-672. ----- (97)
10. Zhang Zhongyi, Wu Ganguo, Guo Jinhui, Zhang Da. Evolution, Migration, Controlling Factors and Forming Setting of Mesozoic Basins in Western Shandong. **ACTA GEOLOGICAL SINICA**, 2005, 79(4), 519-532. ----- (108)
11. YIN Hongfui, TONG Jinnan², ZHANG Kexin². A Review on the Global Stratotype Section and Point of the Permian-Triassic Boundary. **ACTA GEOLOGICA SINICA**, 2005, 715-728. ----- (122)

- 12.Liu Junlai et al. The Liaonan mcc, southeastern Liaoning Province, North China. **Tectonophysics**,2005, 407,65-80.----- (136)
- 13.GONG Yiming,XU Ran,TANG Zhongdao,SI Yuanlan & LI Baohua. Relationships Between bacterial-algal proliferating and mass extinction in the Late Devonian Frasnian-Famennian transition:Enlightening from carbon isotopes and molecular fossils. **Science in China Ser.D Earth Sciences**,2005, Vol.48 No.10 1656-1665. ----- (152)
- 14.LIU Xiangwen, JIN Zhenmin, QU Jing&WANG Lu. Exsolution of ilmenite and Cr-Ti magnetite from oilvine of garnet-wehrlite. **Science in China Ser.D Earth Sciences**,2005, Vol.48 No.9 1368-1376. ----- (162)
- 15.LIU Yongsheng ,GAOShan,WANG Xuance,HU Shenghong&WANG Jianqi. Nb/Ta variations of mafic volcanics on the Archean-Proterozoic boundary:Implications for the Nb/Ta imbalance. **Science in China Ser.D Earth Sciences**,2005, Vol.48 No.8 1106-1119. ----- (171)
- 16.MA Changqian, SHE Zhenbing, XU Pin, WANG Linyan. Silurian A-type granitoids in the southern margin of the Tongbai- Dabieshan: evidence from SHRIMP zircon geochronology and geochemistry. 2005, 48(8): 1134-1145. ----- (185)
- 17.Yong Ge,Qiuming Cheng, Shenyuan Zhang. Reduction of edge effects in spatial information extraction form regional geochemical data:a case study based on multifractal filtering technique.**COMPUTERS&GEOSCIENCES**,2005, 31(2005)545-554. ----- (197)
- 18.JIANPING ZHENG,W. L. GRIFFIN,SUZANNE Y. O'REILLY,J. G. LIOU, R. Y. ZHANG,AND FENGXIANG LU. Late Mesozoic-Eocene Mantle Replacement beneath the Eastern North China Craton: Evidence from the Paleozoic and Cenozoic Peridotite Xenoliths. **International Geology Review**,2005, Vol. 47, 2005, p. 457-472. ----- (207)
- 19.SUO SHUTIAN, ZHONGZENGQIU,ZHOU HANWEN,YOU ZHENDONG,ZHANG HONGFEI,ZHANG LI. Tectonic Evolution of the Dabie-Sulu UHP and HP Metamorphic Belts, East-Central China:Structural Record in UHP Rocks. **International Geology Review**,2005, Vol.47:1207-1221. ----- (223)
- 20.刘祥文、金振民、金淑燕、曲晶、徐薇. 两类榴辉岩的石榴石变形特征差异——来自 TEM 研究的证据. 岩石学报, 2005,1000-0569/2005/021 (02) -0411-20. -- (238)
- 21.刘琰, 邓军, 杨立强, 王庆飞. 异极矿加热过程的研究. 岩石学报,2005, 21(3),993-998. ----- (248)
- 22.刘勇胜、张泽明、Lee Cin-Ty、高山、宗克清. CCSD 主孔高 Ti 榴辉岩非耦合的高 Ti、低 Nb(Zr)特征: 对玄武质岩浆房中磁铁矿分离结晶作用的指示. 岩石学报,2005,1000-0569/2005/021 (02) -0339-46.----- (254)
- 23.欧新功, 金振民, 夏斌, 徐海军, 金淑燕. 超高压变质岩物理性质的相关性对建立结晶岩区地球物理解释标尺的意义. 岩石学报,2005, 1000-0569/2005/021 (03) -1005-14. ----- (262)
- 24.索书田, 钟增球,周汉文, 游振东. 大别-苏鲁区超高压变质岩的多期构造变质演化. 岩石学报,2005, 1000-0569/2005/021 (04) -1175-87.----- (272)
- 25.吴耀、金振民、欧新功、徐海军、王璐. 中国大陆科学钻探(CCS D)主孔地区岩石圈热结构. 岩石学报,2005, 1000-0569/2005/021 (02) -0439-50. ----- (286)
- 26.杨建平, 金振民, 欧新功, 徐海军. 岩石密度和超高压岩石折返速率. 岩石学报,2005, 1000-0569/2005/021 (02) -0427-37.----- (298)
- 27.张静, 燕光谱, 叶霖, 李国平, 李忠烈, 王志光. 河南内乡县银洞沟银多金属矿床碳-氢-氧同

- 位素地球化学. 岩石学报, 2005, 21(5), 1359-1364. ----- (309)
28. 郑建平, 孙敏, 路凤香, 余淳梅, 王方正. 信阳基性麻粒捕虏体及其华北南缘早中生代下地壳性质. 岩石学报, 2005, 1000-0569/2005/021 (01) - 0091-98. ----- (315)
29. 宗克清, 刘勇胜, 高山, 袁洪林, 柳小明, 王选策. 汉诺坝辉石岩包体中单斜辉石的微区微量元素组成特征及其地球动力学意义. 岩石学报, 2005, 1000-0569/2005/021 (02) - 0909-20. ----- (323)
30. Zhang Zhaochong, Mao Jingwen, John J Mahoney, Wang Fusheng and Qu Wenjun. Platinum Group Elements of the Emeishan Large Igneous Province: Implications for mantle plume source. **Geochemical Journal**, 2005, 39(4), 371-382. ----- (335)
31. Cheng, Q. Multifractal Distribution of Eigenvalues and Eigenvectors from 2D Multiplicative Cascade Multifractal Fields. **Mathematical Geology**, 2005, Vol37(8) 915-927. ----- (347)
32. Shen W, Cohen D.R. Fractal models and an application in geochemical exploration. **Mathematical Geology**, 2005, 37(8), 898-913. ----- (360)
33. LI Xuping, LI Yiliang and SHU Guiming. Breakdown of lawsonite subsequent to peak UHP metamorphism in the Dabieterrane and its implication for fluid activity. **Chinese Science Bulletin**, 2005, 50(13), 1366-1372. ----- (379)
34. Liu Junlai et al. Macro- and microscopic mechanical behavior of flow of coal samples. **Chinese Science Bulletin**, 2005, 50(Supp): 59-66. ----- (386)
35. Wu Huaichun, Zhang Shihong, Li Zhengxiang, Li Haiyan and Dong Jin. New Paleomagnetic results from the Yangzhuang Formation of the Jixian System, North China and tectonic implications. **Chinese Science Bulletin**, 2005, 50(14), 1483-1489. ----- (394)
36. ZHENG Jianping, LUO Zhaozhua, YU Chunmei, YU Xiaolu, ZHANG Ruisheng, LU Fengxiang & LI Huimin. Geochemistry and zircon U-Pb ages of granulite xenolith from Tuoyun basalts, Xinjiang: Implications for the petrogenesis and the lower crustal nature beneath the southwestern Tianshan. **Chinese Science Bulletin**, 2005, 2005 Vol.50 No.12 1242-1251. ----- (401)
37. Li Haiyan and Zhang Shihong. Detection of mineralogical changes in pyrite using measurements of temperature-dependence susceptibility. **Chinese Journal of Geophysics**, 2005, 48(6), 1384-1391. ----- (411)

◆ 第二部分 EI 检索论文 ◆

1. Dan-Ping Yan, Mei-Fu Zhou, Yan Wang and Tai-Ping Zhao. The earlier spreading of South China Sea basin resulted by the Late Mesozoic to Early Cenozoic extension of the South China Block? - Structural styles and Chronological evidences from the Dulong-Song Chay tectonic dome. **Earth Science**, 2005, 16(3), 189-199. ----- (419)
2. 邓军, 高帮飞, 王庆飞, 杨立强. 成矿流体系统的形成与演化. 地质科技情报, 2005, 24(1), 49-54. ----- (430)
3. 高山, 周炼, 凌文黎, 刘勇胜, 周鼎武. 华北克拉通南缘太古-元古宙界线安沟群火山岩的年龄及地球化学. 地球科学, 2005, 30(3), 259-263. ----- (436)
4. 刘俊来, 关会梅. 含流体相条件下白云岩的低温流动变形-破裂与溶解-结晶的耦合过程. 矿物岩石, 2005, 25(1), 14-19. ----- (441)

- 5.刘琰, 邓军, 杨立强, 周应华, 高帮飞. 表生异极矿成因研究及其找矿意义. *矿物岩石*, 2005, 25(2), 1-5. ----- (447)
- 6.卢树东, 高文亮, 汪石林, 肖锴, 许建华, 刘健. 江西张十八铅锌矿铅同位素组成特征及其成因意义. *矿物岩石*, 2005, 25(2), 64-69. ----- (453)
- 7.童金南、赵来时、左景勋、Hans J. Hansen, Yuri D. Zakharov. 安徽巢湖地区下三叠统综合层序. *地球科学*, 2005, 30(1), 40-46. ----- (459)
- 8.王晓蕊、高山、柳小明、袁洪林、胡兆初、张宏、王选策. 辽西四合屯早白垩世义县组高镁安山岩的地球化学: 对下地壳拆沉作用和 Sr/Y 变化的指示. *地球科学*, 2005, 35(8): 700-709. ----- (466)
- 9.吴冲龙、刘刚、田宜平. 地矿勘查工作信息化的理论与方法问题. *地球科学*, 2005, 第 30 卷 3 期 359—365 页. ----- (476)
- 10.吴秀玲, 孟大维, 韩郁菁, 韩勇, 郑建平. 大别山双河硬玉石英岩石英中的纳米-亚微米级流体包裹体. *矿物岩石*, 2005, 25(2), 6-9. ----- (483)
- 11.夏庆霖, 陈永清, 卢映祥, 蒋成兴, 刘红光, 吕志成. 云南芦子园铅锌矿床地球化学、流体包裹体及稳定同位素特征. *地球科学*, 2005, 2005, 30(2), 177-186. ----- (487)
- 12.张利, 钟增球, 张宏飞, 王林森. 桐柏一大别造山带高压变质单元岩石 Pb 同位素组成. *地球科学*, 2005, 30(6), 729-737. ----- (497)
- 13.张利, 钟增球, 张宏飞, 王林森. 从 Pb 同位素组成看东秦岭官坡超高压变质岩片的走势. *矿物岩石*, 卷 25, 期 2, 总 100, 页 60—63, 2005, 6. ----- (506)
- 14.张招崇, 闫升好, 陈柏林, 周刚, 何永康, 柴凤梅, 何立新. 阿尔泰造山带南缘中泥盆世苦橄岩及其大地构造和岩石学意义. *地球科学*, 2005, 30(3), 289-297. ----- (510)
- 15.赵来时, 童金南, Orchard m.J., 左景勋. 安徽巢湖地区下三叠统牙形石生物地层分带及全球对比. *地球科学*, Vol.30 No.5 Sept. 2005. ----- (519)
- 16.钟玉芳, 马昌前, 余振兵, 林广春, 续海金, 王人镜, 杨坤光, 刘强. 江西九岭花岗岩类复式岩基锆石 SHRIMP U-Pb 年代学. *地球科学*, 2005, 30(6), 685-691. ----- (531)

◆ 第三部分 其它类别论文 ◆

- 1.Gregory A. DAVIS. THE LATE JURASSIC "TUCHENGZI/HOUCHENG" FORMATION OF THE YANSHAN FOLD-THRUST BELT: AN ANALYSIS. *Earth Science Frontiers*, 2005, 12(4): 331-345. ----- (539)
- 2.WANG Jizhong, LI Shengrong, JIANG Yonghong, WEI Ruihua and NIU Huapeng. Environmental properties of metallic minerals and their applications in environmental protection in China. **CHINESE JOURNAL OF GEOCHEMISTRY**, 2005, 24(3), 221-227. ----- (554)
- 3.Wu Huaichun, Zhang Shihong, Jiang Ganqing and Li Haiyan. Magnetic susceptibility variations of the Ediacaran cap carbonates in the Yangtze platform and their implications for paleoclimate. **Chinese Journal of Oceanology and Limnology**, 2005, 23(3), 291-298. ----- (561)
- 4.柴凤梅, 张招崇, 毛景文, 董连慧, 张作衡. 岩浆型 Cu-Ni-PGE 硫化物矿床研究的几个问题探讨. *矿床地质*, 2005, 24(3), 325-335. ----- (569)
- 5.邓军, 王庆飞, 高帮飞, 黄定华, 杨立强, 徐浩, 周应华. 鄂尔多斯盆地演化与多种能源矿产分布. *现代地质*, 19(4), 538-545. ----- (580)
- 6.邓军, 王庆飞, 黄定华, 高帮飞, 杨立强, 徐浩. 鄂尔多斯盆地基底演化及其对盖层控制作用. *地学前缘*, 2005, 12(3), 91-99. ----- (588)
- 7.狄永军, 赵海玲, 吴淦国, 张达, 藏文拴, 刘清华. 铜陵地区燕山期侵入岩成因与三端元岩浆混

- 合作用. 地质论评, 2005, 51(5), 528-538. ----- (597)
8. 高金汉, 王训练, 乔子真. 北祁连山东部早石炭世早期腕足动物群落的古地理意义. 古地理学报, 2005, 7(4), 493-502. ----- (608)
 9. 龚一鸣, 胡斌, 齐永安, 张国成. 遗迹学的研究现状与新进展——第 8 届国际遗迹组构专题研讨会综述. 古地理学报, Vol.7 No.4 2005. ----- (618)
 10. 何谋春, 吕新彪, 姚书振, 刘艳荣, 樊五杰. 沉积岩中残留有机质的拉曼光谱特征. 地质科技情报, 2005 年 9 月 第 24 卷 第 3 期. ----- (624)
 11. 侯青叶, 赵志丹, 张宏飞, 张本仁, 陈岳龙. 北祁连玉石沟蛇绿岩印度洋 MORB 型同位素组成特征及其地质意义. 中国科学 D 辑, 2005, 35(8), 710-719. ----- (628)
 12. 江永宏, 李胜荣. 湘、黔地区前寒武—寒武纪过渡时期硅质岩生成环境研究. 地学前缘, 2005, 12(4), 622-629. ----- (638)
 13. 李海燕, 张世红. 黄铁矿加热过程中的矿相变化研究—基于磁化率随温度变化特征分析. 地球物理学报, 2005, 48(6), 1384-1391. ----- (646)
 14. 李胜荣, 肖润, 周肃, 莫宣学, 申俊峰, 闫柏琨, 刘波. 西藏改则地区金成矿作用. 现代地质, 2005, 24(1), 1-14. ----- (654)
 15. 李祯, 李胜荣, 申俊峰, 霍晓君, 佟景贵, 王对兴, 罗军燕. 粉煤灰和城市污泥配施对荒漠土壤持水性能影响的实验研究. 地球与环境, 2005, 33(2): 74-78. ----- (668)
 16. 刘和甫, 李晓清, 刘立群, 李小军, 胡少华. 成藏区带地球动力学与远景圈闭. 地学前缘, 2005, 12(4), 468-479. ----- (673)
 17. 刘家军, 李志明, 刘建明, 王建平, 冯彩霞, 卢文全. 自然界中的辉锑矿-硒锑矿矿物系列. 吉林大学学报(地球科学版), 2005, 35(5), 545-553, 563 ----- (685)
 18. 刘家军, 冯彩霞, 李志明, 王建平, 刘世荣, 周国富. 湖北渔塘坝硒矿床中次生自然硒的特征与意义. 现代地质, 2005, 19(4): 531-537. ----- (695)
 19. 刘俊来, 杨光, 马瑞. 高温高压实验变形煤流动的宏观与微观力学表现. 科学通报, 2005, 50 (增刊): 56-63. ----- (702)
 20. 刘少峰, 王陶, 张会平, 程三友, 孙亚平, 雷国静. 数字高程模型在地表过程研究中的应用. 地学前缘, 2005, 12(1), 303-309. ----- (710)
 21. 刘少峰. 张国伟. 盆山关系研究的基本思路、内容和方法. 地学前缘, 2005, 12 (3), 101-111. ----- (717)
 22. 刘琰, 邓军, 蔡克勤, 周彦, 王庆飞, 周应华, 高帮飞, 李德秀, 徐福玉, 朱悦荣. 四川平武板状绿帘角闪岩矿物学特征及板状成因. 地学前缘, 2005, 12(2), 324-331. ----- (728)
 23. 刘琰, 邓军, 蔡克勤, 朱友楠, 王庆飞, 周应华, 高帮飞. 云南兰坪富锑文石的振动光谱特征. 岩石矿物学杂志, 24 (2), 110-116. ----- (736)
 24. 刘琰, 邓军, 王庆飞, 周应华. 云南金顶异极矿晶体化学特征与颜色成因探讨. 高校地质学报, 2005, 11 (3), 434-441. ----- (743)
 25. 柳小明, 高山, 凌文黎, 袁洪林, 胡兆初. 扬子克拉通 35 亿年碎屑锆石的发现及地质意义. 自然科学进展, 2005 年 11 月 第 15 卷 第 11 期. ----- (751)
 26. 吕军, 王建民, 岳帮江, 王洪波, 于荣文, 赵立国. 三道湾子金矿床流体包裹体及稳定同位素地球化学特征. 地质与勘探, 2005, 41(3): 33-37. ----- (755)
 27. 吕万军, I-Ming Chou, Robert C. Burruss, 金庆焕, 傅家谟. 拉曼光谱原位观测水合物形成后的饱和甲烷浓度. 地球化学, 2005, Vol.34, No.2, 187-192. ----- (760)
 28. 梅冥相, 马永生, 邓军, 李浩, 郑宽兵. 加里东运动构造古地理及滇黔桂盆地的形成—兼论滇黔桂盆地深层油气勘探潜力. 地学前缘, 2005, 12(3): 227-236. ----- (766)

- 29.梅冥相, 马永生, 邓军, 张海, 孟晓庆, 陈永红, 聂瑞贞, 张从.上扬子区下古生界层序地层格架的初步研究. 现代地质,2005, 19(4):,551-562. ----- (776)
- 30.孟大维, 孙凡, 陈维毅, 郑建平. 大别山超高压变质矿物中的微结构缺陷及其意义.电子显微学报, 2005 年第 24 卷 第 4 期 P322. ----- (788)
- 31.莫宣学, 董国臣, 赵志丹, 周肃, 王亮亮, 邱瑞照, 张凤琴. 西藏冈底斯带花岗岩的时空分布特征及地壳生长演化信息. 高校地质学报, 2005,11(3),281-290. ----- (789)
- 32.史玉芳, 肖少泉, 卢 练. 镍-钴合金块状样品的 X 射线荧光光谱分析.理化检验—化学分册, 2005 年 第 41 卷 增刊. ----- (799)
- 33.童金南,Hans J. Hansen,赵来时, 左景勋. 印度阶—奥伦尼克阶界线层型候选剖面——安徽巢湖平顶山西剖面地层序列. 地层学杂志, 2005 年 4 月第 29 卷 第 2 期.----- (800)
- 34.童金南,王德珏. 三叠纪年代地层与生物复苏. 地球科学进展, 2005,20 (12): 1321-1326. ----- (810)
- 35.万丽, 王庆飞, 高帮飞, 王颖, 周应华, 徐浩. 成矿预测数据统计方法. 现代地质,2005, 19(4),615-620.----- (816)
- 36.万晓樵, 高莲凤, 李国彪, 陈文, 张彦. 西藏江孜-浪卡子一带的侏罗—白垩纪界线地层. 现代地质,2005, 19(4): 479-487. ----- (822)
- 37.汪昌亮, 丛卫克, 颜丹平, 周美夫, 董铁柱, 朱忠, 卞雄飞. 赣北程浪断裂带的形成: 程浪超基性岩墙群和星子花岗岩的地球化学证据. 现代地质, 2005,19(3),325-333. ----- (831)
- 38.汪新伟, 汪新文, 刘剑平, 马永生.准噶尔盆地南缘褶皱-逆冲断层带分析.地学前缘,2005, 12(4), 411-421. ----- (840)
- 39.王长明, 邓军, 张寿廷, 燕长海. 河南卢氏—栾川地区铅锌矿成矿多样性分析及成矿预测. 地质通报,2005, 24(10-11): 1074-1080. ----- (851)
- 40.王翠芝, 肖荣阁, 贾琇明, 周红春, 刘军. 山东淄博铝土矿地质特征及成矿作用. 地质与勘探,2005, 41(5),34-37. ----- (858)
- 41.王吉中, 李胜荣, 刘宝林, 佟景贵. 国内矿物冶—重金属废水研究进展与展望. 矿物岩石地球化学通报,2005, 24(2): 159-164. ----- (862)
- 42.王丽娟, 鲁安怀, 王长秋, 郑喜珊, 赵东军, 刘瑞. 纳米纤维状白炭黑的孔隙特征. 岩石矿物学杂志,2005, 24 卷 6 期. P515-520.----- (868)
- 43.王庆飞, 邓军, 黄定华, 高帮飞, 徐浩. 鄂尔多斯盆地石炭纪中央古隆起形成机制. 现代地质,2005, 19 (4) ,546-551. ----- (874)
- 44.王庆飞. 邓军. 黄定华. 铜陵矿集区构造-岩浆-成矿系统解析. 地学前缘,200512 (3) . -- ----- (880)
- 45.韦延光, 邓军, 王建国, 张志启, 闫顺令, 辛洪波, 尤世娜. 谢家沟剪切带蚀变岩型金矿床地质特征及成因初步探讨. 黄金,2005, 26(4): 8-12. ----- (881)
- 46.韦延光, 王建国,邓军, 张志启, 林吉照, 闫顺令. 山东谢家沟金矿流体包裹体研究及其地质意义. 现代地质,2005, 19(2): 224-230. ----- (886)
- 47.吴怀春, 张世红, 李正祥, 李海燕, 董进. 华北地台蓟县系杨庄古地磁新结果及其大地构造意义. 科学通报,2005, 50(13), 1370-1376. ----- (893)
- 48.吴秀玲, 樊孝玉, 刘忠, 韩勇, 郑建平. 安徽双河超高压变质岩矿物包裹体的精细结构及其地质意义. 电子显微学报, 2005 年第 24 卷 第 4 期 P321. ----- (900)
- 49.肖少泉,史玉芳,姚正学,吴百一. SRS303 X 射线荧光光谱仪的故障维修三例.理化检验—化学分册, 2005 年 第 41 卷 增刊. ----- (901)
- 50.肖少泉,吴百一. JSM-35CF 扫描电子显微镜故障维修三例. 电子显微学报, 2005 年第 24 卷 第 4 期 P391. ----- (903)

51. 谢桂青, 毛景文, 胡瑞忠, 李瑞玲, 曹建劲. 中国东南部中—新生代地球动力学背景若干问题的探讨. 地质论评, 2005, 51(6): 613-620. ----- (904)
52. 闫柏琨, 王润生, 甘甫平, 刘圣伟, 杨苏明, 陈伟涛, 唐攀科. 热红外遥感岩矿信息提取研究进展. 地球科学进展, 2005, 20(10): 1116-1126. ----- (912)
53. 余心起, 吴淦国, 张达, 狄永军, 藏文拴, 张祥信, 汪群峰. 中国东南部中生代构造体制转换作用研究进展. 自然科学进展, 2005, 15(10): 1167-1173. ----- (923)
54. 喻学惠, 赵志丹, 莫宣学, 周肃, 朱德勤, 王永磊. 甘肃西秦岭新生代钾霞黄长岩的 $^{40}\text{Ar}/^{39}\text{Ar}$ 同位素定及地质意义. 科学通报, 2005, 50(23), 2638-2643. ----- (931)
55. 张达, 吴淦国, 彭润民, 吴建设, 狄永军, 张祥信, 汪群峰. 闽中地区马面山群东岩组变质岩形成的古构造环境研究. 地学前缘, 2005, 12(1): 311-320. ----- (937)
56. 张招崇, 王福生, 曲文俊, 郝艳丽, John J. MAHONEY. 峨嵋山大火成岩省中高 Os 苦橄岩的发现及地质意义. 地质学报, 2005, 79(4): 515-521. ----- (948)
57. 郑建平. 捕虏体麻粒岩锆石年龄和铅同位素: 华北地块下地壳的形成与再造. 矿物岩石地球化学通报, Vol.24 No.1, 2005 Jan. ----- (955)
58. 郑建平, 罗照华, 余淳梅, 余晓露, 张瑞生, 路凤香, 李惠民. 新疆托云麻粒岩捕虏体地球化学和锆石年代学: 岩石成因及西南天山下地壳性质. 科学通报, 2005, 50(8), 793-801. ----- (965)
59. 周学武, 李胜荣, 鲁力, 李俊建, 王吉中. 辽宁丹东五龙区石英脉型金矿床的黄铁矿标型特征研究. 现代地质, 2005, 19(2): 231-238. ----- (974)

◆ 第四部分 专著 ◆

1. Zhao Laishi, Tong Jinnan and Mike Orchard. Study on the Lower Triassic Conodont Sequence and the Induan-Olenekian Boundary in Chaohu, Anhui Province. China University of Geosciences Press Wuhan, Hubei, China. -- (983)
2. 郝芳. 超压盆地生烃作用动力学与油气成藏机理. 科学出版社出版 ----- (984)
3. 张克信. 中华人民共和国区域地质调查报告—煤山镇幅、长兴县幅. 中国地质大学出版社. ----- (985)
4. 路凤香、吴其反等. 中国东部典型地区下部岩石圈组成、结构和层圈相互作用. 中国地质大学出版社. ----- (986)
5. Cheng, Q. GIS based fractal/multifractal anomaly analysis for modeling and prediction of mineralization and mineral deposits, in Jeff Harris (ed.). GIS Applications in Earth Sciences, Geological Association of Canada Special Book. ----- (987)
6. Thiart, C., Bonham-Carter, G.F., Agterberg, F.P., Cheng, Q., and Panahi, A. An application of the new Omnibus test for conditional independence in weights-of-evidence modeling, in Jeff Harris (ed.) GIS Applications In Earth Sciences, Geological Association of Canada Special Book ----- (989)

◆ 第五部分 会议论文简表 ◆

▲ 中国—巢湖三叠纪年代地层与生物复苏国际学术会议

1. Hansen, Hans J. Hansen, Tong Jinnan. Lower Triassic Magnetostratigraphy in Chaohu. Albertiana, 2005, vol.1, 36-37.

2. Tong Jinnan, *Douglas H. Erwin*, Zuo Jinxun, Zhao Laishi. Lower Triassic Carbon Isotope Stratigraphy in Chaohu, Anhui: Implication to Biotic and Ecological Recovery. *Albertiana*, 2005, vol.1, 75-76.
3. Zhao Laishi, *Mike Orchard*, Tong Jinnan. Conodont Sequences and its Global Correlation of the Induan-Olenekian Boundary in West Pingdingshan Section, Chaohu, Anhui Province. *Albertiana*, 2005, vol.1, 108-111.
4. Zhao Laishi, Tong Jinnan, *Mike Orchard*, *Chen Bing* and *Huang Xiaogang*. An Intercalibrated Permian and Lower Triassic of the Guimenguan Section, South Chaohu, Anhui Province. *Albertiana*, 2005, vol.1, 111-113.
5. Zhao Laishi, *Xiong Xinqi*, *Yang Fengqing*, *Wang Zhiping*, and *He Weihong*. Conodonts from the Lower Triassic in the Nantuowan Section of Daxiakou, Xingshan Country, Hubei Province. *Albertiana*, 2005, vol.1, 113-115.
6. Zhao Laishi. Permian-Triassic Sequences in Meishan and Hushan, Lower Yangtze, Guide to Pre-Symposium Field Excursion of the International Symposium on the Triassic Chronostratigraphy and Biotic Recovery. *Albertiana*, 2005, vol.2, 119-128.
7. Tong Jinnan, Zhao Laishi. Triassic in Chaohu, Anhui Province, Guide to Mid-Symposium Field Excursion of the International Symposium on the Triassic Chronostratigraphy and Biotic Recovery. *Albertiana*, 2005, vol.2, 129-138.

▲ 国际数学地质协会 IAMG2005 年会, ISTP 收录

8. Yong Ge, Yunyan Du, Qiuming Cheng. Multifractal Filtering Method for Extraction of Ocean Eddies from Remotely Sensed Image. *Proceedings of IAMG'05 GIS and Spatial*, vol.1, 74-79.
9. Guangdao Hu, Xing Liu. Imaged Geological Map - A Quantitative Way to Express Geological Information. *Proceedings of IAMG'05 GIS and Spatial*, vol.1, 139-144.
10. Shouting Zhang, Pengda Zhao, Qinglin Xia, Huashan Sun, Mangen Li. The Ore-forming Spectrum and Multitarget Minerals Prediction and Assessment of the Himalayan Alkali-rich Porphyry in Northwestern Yunnan Province. *Proceedings of IAMG'05 GIS and Spatial*, vol.1, 145-150.
11. Hongbo Mei, Guangdao Hu, Dingping Li, Xing Liu. Study on Information Query System Based on GIS for Mineral Producing Areas of Yunnan Province, China. *Proceedings of IAMG'05 GIS and Spatial*, vol.1, 167-170.
12. Chunfang Kong, Kai Xu, Chonglong Wu, Shaohu Li, Jin Liu. The Study on Classifying and Extracting the Urban Land-use Information High-Resolution Image Based on the Multi-Characteristics of the Objects. *Proceedings of IAMG'05 GIS and Spatial*, vol.1, 237-242.
13. Chonglong Wu, Yiping Tian, Xiaoping Mao, Shaohu Li, Xing Li, Gang Liu. Zhengping Weng. Theory and Approach of Three Dimensional Visualization Modeling of Structure-Stratigraphic Framework of Basins. *Proceedings of IAMG'05 GIS and Spatial*, vol.1, 279-284.
14. Qiuming Cheng. Multiplicative Cascade Mineralization Processes and Singular Distribution of Mineral Deposit Associated Geochemical Anomalies. *Proceedings of IAMG'05 GIS and Spatial*, vol.1, 297-302.
15. Li Cao, Qiuming Cheng. A Tentative Integrated Model of Scale Invariant Generator Technique (SIG) and Spectrum-Area (S-A) Technique. *Proceedings of IAMG'05 GIS and Spatial*, vol.1, 303-309.
16. Shuyun Xie, Zhengyu Bao, Deyi Xu. Geochemical Multifractal Distribution Patterns in Soils and its Implication for the Environmental Assessment. *Proceedings of IAMG'05 GIS and Spatial*, vol.1, 310-316.
17. Zhijing Wang, Qiuming Cheng, Qinglin Xia, Zhijun Chen. The P-A Fractal Model Charactering Microtexture Properties of Minerals. *Proceedings of IAMG'05 GIS and Spatial*, vol.1, 317-322.

18. Qiuming Cheng. Multifractal Modeling of Hydrothermal Mineralization: Sn Deposit Prediction in Gejiu Mineral District, Yunnan, Southwestern China. Proceedings of IAMG'05 GIS and Spatial, vol.1, 446–451.
19. Qingmou Li, Qiuming Cheng. A GIS-based W-A Fractal Model for Extracting Spatial Information from Geophysical and Geochemical Data. Proceedings of IAMG'05 GIS and Spatial, vol.1, 470–474.
20. Zhijun Chen, Qiuming Cheng, Jianguo Chen. Significance of Fractal Measure in Local Singularity Analysis of Multifractal Model. Proceedings of IAMG'05 GIS and Spatial, vol.1, 475–480.
21. Qingmou, Qiuming Cheng. Nonlinear Geochemical Series Analysis in an Experimental Orthogonal Function Space –a Multifractal Singular-Spectrum-Analysis Model (M-SSA) and its Application. Proceedings of IAMG'05 GIS and Spatial, vol.1, 493–498.
22. Gang Liu, Chonglong Wu, Weizhong Li, Xinqing Wang, Xialin Zhang. GeoSurvey: a Computer-Aided Geological Survey System Based on Multi-S Integration and Tablet Portable Computer. Proceedings of IAMG'05 GIS and Spatial, vol.2, 898–903.
23. Xinqing Wang, Wenxia Zhao, Renguang Zuo, Xiaogang Ma. Three-related Geology Observing Point Model in Computer-aided Regional Geological Survey. Proceedings of IAMG'05 GIS and Spatial, vol.2, 917–922.
24. Chonglong Wu, Gang Liu, Yiping Tian, Xiaoping Mao, Xinqing Wang, Xialin Zhang. GeoView: A Computer-Aided System for Informalization of Geological and Mineral Resources Survey and Exploration Works. Proceedings of IAMG'05 GIS and Spatial, vol.2, 958–963.
25. Zhenwen He, Chonglong Wu, Yiping Tian, Ming Xiong, Xialin Zhang. Dynamic Multi Source Spatial Data Collection and Object-Oriented Grid Storage Framework of Digital Yangtze. Proceedings of IAMG'05 GIS and Spatial, vol.2, 970–975.
26. Xiaogang Ma, Chonglong Wu, Xinqing Wang, Yongqing Chen, Yong Wang. Centralized Management Approach and Database Development of Multisource Geoscientific Information. Proceedings of IAMG'05 GIS and Spatial, vol.2, 1006–1011.
27. Qinglin Xia, Pengda Zhao, Shouting Zhang, Huashan Sun. GIS Spatial-Temporal Model of Geological Anomaly: A Case for Cenozoic Geology in Northwestern Yunnan Province, China. Proceedings of IAMG'05 GIS and Spatial, vol.2, 1111–1116.
28. Yiping Tian, Xiaoping Mao, Shaohu Li, Zhengping Weng, Chonglong Wu. Application of GIS in Basin Modelling. Proceedings of IAMG'05 GIS and Spatial, vol.2, 1147–1152.

The rate of change of EOF1 has a unimodal distribution with a long tail, indicative of rapid melting. Terminations are defined to initiate when the rate of change in EOF1 first exceeds the two-standard-deviation level. This criterion identifies each of the usual terminations^{10,11} and two events in the termination 3 deglacial sequence (termed 3a and 3b for the younger and older events, respectively). Additional rules could be added to exclude 3a or 3b, but this rejection seems ad hoc, and so we use all eight termination events. Note, the timing of termination 3 predicted by the Paillard model¹ also coincides with either event 3a or 3b, depending on slight changes in the parameterizations. Reassuringly, results are not sensitive to details of the test: either termination 3a or 3b can be excluded; termination times can be defined using the midpoint between the local minimum and maximum bracketing each termination; and individual benthic or planktic $\delta^{18}\text{O}$ records¹⁵ can be used in place of EOF1.

The probability density function (PDF) associated with H_0 is estimated using the modified random-walk model (equation (1)). A realization of R is obtained by sampling the phase of obliquity at eight consecutive termination initiations, generated from equation (1), and the PDF of H_0 is estimated by binning 10^4 such realizations of R . Other methods are to assume a uniform phase distribution, use surrogate data techniques³⁰, or to derive statistics from ensemble runs of other models, but all of these give PDF estimates which make H_0 more easily rejected and are therefore not used.

To estimate the PDF associated with H_1 , we assume that glacial terminations always occur at the same phase of obliquity, but that the phase observations are subject to identification and age-model error. A Monte Carlo technique is used where the timing of the glacial terminations are perturbed according to the estimated age uncertainties¹³ (these average ± 9 kyr) and identification error (± 1 kyr, the EOF1 sampling resolution). A realization of R is then computed using the phase of obliquity at the perturbed ages, and 10^4 such realizations are binned to estimate the PDF of H_1 . We estimate the likelihood of correctly rejecting H_0 (that is, the power of the obliquity test) to be 0.57. See the Supplementary Information for a listing of the other pertinent data and statistics.

Received 6 August 2004; accepted 24 January 2005; doi:10.1038/nature03401.

- Hays, J., Imbrie, J. & Shackleton, N. Variations in the earth's orbit: Pacemaker of the ice ages. *Science* **194**, 1121–1132 (1976).
- Imbrie, J. & Imbrie, J. Modeling the climatic response to orbital variations. *Science* **207**, 943–953 (1980).
- Paillard, D. The timing of Pleistocene glaciations from a simple multiple-state climate model. *Nature* **391**, 378–391 (1998).
- Liu, H. Insolation changes caused by combination of amplitude and frequency modulation of the obliquity. *J. Geophys. Res.* **104**, 25197–25206 (1999).
- Gildor, H. & Tziperman, E. Sea ice as the glacial cycles' climate switch: Role of seasonal and orbital forcing. *Paleoceanography* **15**, 605–615 (2000).
- Saltzman, B. Stochastically-driven climatic fluctuations in the sea-ice, ocean temperature, CO_2 , feedback system. *Tellus* **34**, 97–112 (1982).
- Pelletier, J. Coherence resonance and ice ages. *J. Geophys. Res.* **108**, doi:10.1029/2002JD003120 (2003).
- Wunsch, C. The spectral description of climate change including the 100ky energy. *Clim. Dyn.* **20**, 353–363 (2003).
- Saltzman, B. *Dynamical Paleoclimatology: Generalised Theory of Global Climate Change* (Academic, San Diego, 2002).
- Broecker, W. Terminations. in *Milankovitch and Climate* (eds Berger, A. et al.) Part 2, 687–698 (D. Riedel, Hingham, 1984).
- Raymo, M. E. The timing of major climatic terminations. *Paleoceanography* **12**, 577–585 (1997).
- Milankovitch, M. *Kanon der Erdbestrahlung und seine Anwendung auf das Eiszeitenproblem* (Royal Serbian Academy, Belgrade, 1941).
- Huybers, P. & Wunsch, C. A depth-derived Pleistocene age-model: Uncertainty estimates, sedimentation variability, and nonlinear climate change. *Paleoceanography* **19**, doi:10.1029/2002PA000857 (2004).
- Imbrie, J. et al. in *Milankovitch and Climate* (eds Berger, A. et al.) Part 1, 269–305 (D. Riedel Publishing Company, 1984).
- Shackleton, N. J., Berger, A. & Peltier, W. R. An alternative astronomical calibration of the lower Pleistocene timescale based on ODP site 677. *Trans. R. Soc. Edinb. Earth Sci.* **81**, 251–261 (1990).
- Roe, G. & Allen, M. A comparison of competing explanations for the 100,000-yr ice age cycle. *Geophys. Res. Lett.* **26**, 2259–2262 (1999).
- Blunier, T. & Brook, E. Timing of millennial-scale climate change in Antarctica and Greenland during the last glacial period. *Science* **291**, 109–112 (2001).
- Wunsch, C. Greenland-Antarctic phase relations and millennial time-scale climate fluctuations in the Greenland cores. *Quat. Sci. Rev.* **22**, 1631–1646 (2003).
- Marshall, S. & Clark, P. Basal temperature evolution of North American ice sheets and implications for the 100-kyr cycle. *Geophys. Res. Lett.* **29**, doi:10.1029/2002GL015192 (2002).
- Zwally, H. et al. Surface melt-induced acceleration of greenland ice-sheet flow. *Science* **297**, 218–222 (2002).
- Rubincam, D. Insolation in terms of earth's orbital parameters. *Theor. Appl. Climatol.* **48**, 195–202 (1994).
- Huybers, P. & Wunsch, C. Rectification and precession-period signals in the climate system. *Geophys. Res. Lett.* **30**, doi:10.1029/2003GL017875 (2003).
- Raymo, M. & Nisancioglu, K. The 41 kyr world: Milankovitch's other unsolved mystery. *Paleoceanography* **18**, doi:10.1029/2002PA000791 (2003).
- Berger, A. & Loutre, M. F. Astronomical solutions for paleoclimate studies over the last 3 million years. *Earth Planet. Sci. Lett.* **111**, 369–382 (1992).
- Huybers, P. *On the Origins of the Ice Ages: Insolation Forcing, Age Models, and Nonlinear Climate Change*. PhD thesis, MIT (2004).
- Wunsch, C. Quantitative estimate of the Milankovitch-forced contribution to observed quaternary climate change. *Quat. Sci. Rev.* **23**, 1001–1012 (2004).

- Ruddiman, W. F. Orbital insolation, ice volume, and greenhouse gases. *Quat. Sci. Rev.* **22**, 1597–1622 (2003).
- Upton, G. & Fingleton, B. *Spatial Data Analysis by Example Vol. 2* (John Wiley and Sons, Chichester, 1989).
- Rosenblum, M. & Pikovsky, A. Synchronization: from pendulum clocks to chaotic lasers and chemical oscillators. *Contemp. Phys.* **44**, 401–416 (2003).
- Schreiber, T. & Schmitz, A. Surrogate time series. *Physica D* **142**, 346–382 (2000).

Supplementary Information accompanies the paper on www.nature.com/nature.

Acknowledgements Useful comments were provided by E. Boyle, W. Curry, T. Herbert, J. McManus, F. Ng, M. Tingley and G. Yang. P.H. is supported by the NOAA Postdoctoral Program in Climate and Global Change and C.W. is supported in part by the National Ocean Partnership Program (ECCO).

Competing interests statement The authors declare that they have no competing financial interests.

Correspondence and requests for materials should be addressed to P.H. (phuybers@whoi.edu).

Two episodes of microbial change coupled with Permo/Triassic faunal mass extinction

Shucheng Xie^{1,2}, Richard D. Pancost¹, Hongfu Yin², Hongmel Wang³ & Richard P. Evershed¹

¹Organic Geochemistry Unit, Bristol Biogeochemistry Center, School of Chemistry, University of Bristol, Cantock's Close, Bristol BS8 1TS, UK

²Faculty of Earth Science and State Key Laboratory of Geological Processes and Mineral Resources, China University of Geosciences, Wuhan 430074, People's Republic of China

³School of Environmental Studies, China University of Geosciences, Wuhan 430074, People's Republic of China

Microbial expansion following faunal mass extinctions in Earth history can be studied by petrographic examination of microbialites (microbial crusts)^{1,2} or well-preserved organic-walled microbes³. However, where preservation is poor, quantification of microbial communities can be problematic. We have circumvented this problem by adopting a lipid biomarker-based approach to evaluate microbial community changes across the Permo/Triassic (P/Tr) boundary at Meishan in South China. We present here a biomarker stratigraphic record showing episodic microbial changes coupled with a high-resolution record of invertebrate mass extinction. Variation in the microbial community structure is characterized by the 2-methylhopane (2-MHP) index (a ratio of the abundance of cyanobacterial biomarkers to more general bacterial biomarkers). Two episodes of faunal mass extinction were each preceded by minima in the 2-MHP index, followed by strong maxima, likely reflecting microbial responses to the catastrophic events that caused the extinction and initiated ecosystem changes. Hence, both cyanobacterial biomarker and invertebrate fossil records provide evidence for two episodes of biotic crisis across the P/Tr boundary.

In bacteria, bacteriohopanepolyols (BHPs) are amphiphilic biochemicals that serve regulatory and rigidifying functions in cell membranes. It has been demonstrated that the cyanobacterial lineage currently comprises the only known quantitatively significant source of 2-methyl-BHPs^{4–6}, such that the presence of abundant 2 α -methylhopanes (2-MHPs) derived from 2-methyl-BHP precursors is believed to be characteristic of cyanobacteria⁴. This is particularly true for 2-methyl-BHPs containing more than 32 carbon atoms, which have not been detected in organisms other

than cyanobacteria⁴. Thus, the 2-MHP index, which is the ratio of 2-MHPs to hopanes lacking additional methyl substituents (HPs, derived from a range of bacteria, including cyanobacteria⁷), provides insight into the cyanobacterial component of the bacterial population.

We have conducted a survey of microbial biomarkers in sedimentary rocks spanning the P/Tr boundary (which is characterized by the most severe biotic crisis of the Phanerozoic) and compared these biomarkers to faunal extinction patterns. We targeted the Meishan sections in South China for several reasons. First, they contain well established, high-resolution faunal stratigraphic distributions that are well dated⁸, thereby allowing comparison of the fossil biomarker record with macro- and micro-fossil records. Second, they are the most extensively studied P/Tr boundary sections anywhere in the world⁸ and are where the Global Stratotype Section and Point (GSSP) was recently defined⁹. Third, they are the location at which the rapid nature of biotic crises has been proposed⁸. Finally, they possess organic matter that is relatively thermally immature, as indicated by T_{max} values of 424–466 °C (temperature of maximum pyrolysis yield in Rock-Eval pyrolysis; see Supplementary Table 1), making it possible to investigate biomarkers.

The 2-MHP indices were determined by gas chromatography/mass spectrometry (GC/MS) of the saturated hydrocarbon fraction of solvent extracts of the sedimentary rocks. 2-MHP indices range from 1.2% to 6.6%, consistent with previously reported values for the Paleozoic⁴. In general, values are between 2.0% and 3.3%, but the record is characterized by two minima (with values of 1.2–1.7%) at bed 24e (extending to the bottom of bed 25) and beds 27–28; each of these is followed by a dramatic maximum (6.6%) at beds 26 and 29, respectively (Fig. 1). These maxima indicate at least two major shifts in the cyanobacterial community, either through changes in the cyanobacterial species composition (because not all cyanobacteria biosynthesize 2-methyl-BHPs) or an increase in the size of the total cyanobacterial community. Although an alternative explanation is that changes in the 2-MHP depth profile record varying abundances of a less common 2-MHP producer, this is unlikely because these episodes are also associated with enhanced relative abundances of more diagnostic 2-MHPs with extended side chains, including the C_{32} 22R and 22S isomers^{4,10}.

Other than changes in cyanobacterial community structure, the increase in 2-MHP indices could be caused by differences in either thermal maturity or lithology/facies. The former is unlikely given the narrow stratigraphic range, confirmed by the weak correlation

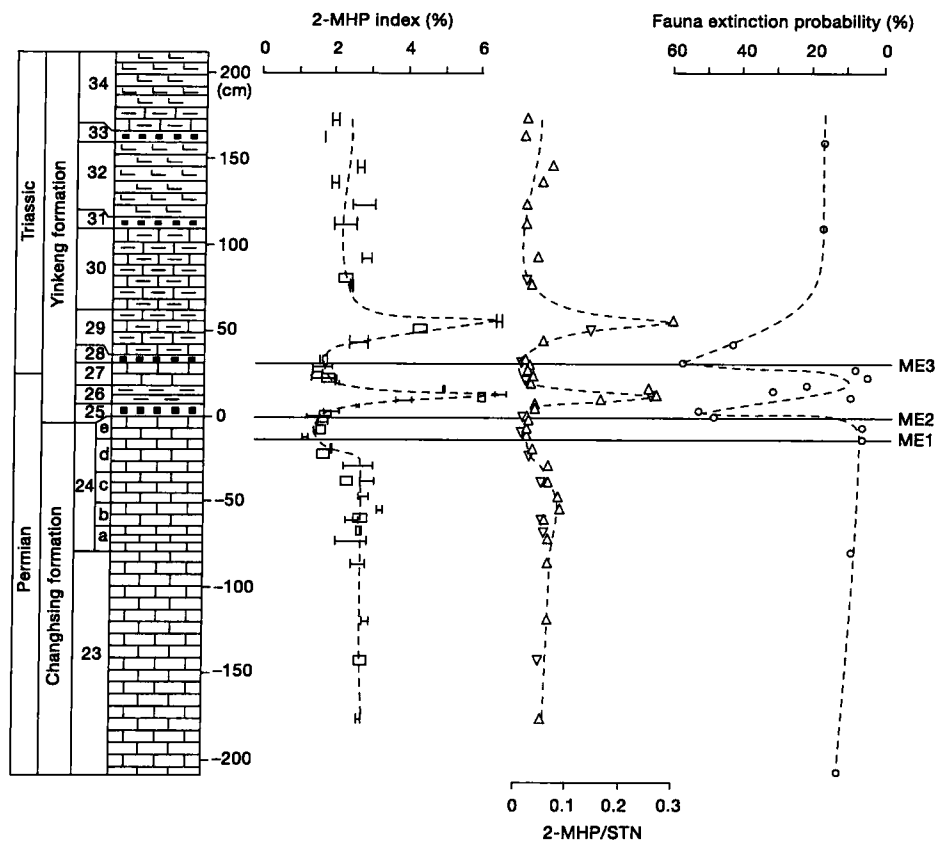


Figure 1 Profiles of the lithology, 2-MHP indices, the ratio of 2-MHP to steranes (2-MHP/STN) and the extinction probability of marine invertebrates across the P/Tr boundary at the Meishan sections in Zhejiang, South China. The lithology of the studied profiles near the P/Tr boundary includes lime mudstones (beds 23, 24), pale-coloured, alternated ash clay beds (beds 25, 28, 31, 33), a laminated organic-rich calcareous claystone (bed 26), a lime mud bed (bed 27), and grey organic-rich shales, pale marls or muddy limestone (beds 29, 30, 32, 34). The high-resolution 2-MHP indices are from Meishan Section B and C (the error bars reflect the error: 2σ of >3 measurements). The ratio of 2-MHP to steranes is the abundance of C_{31} 2-MHP relative to C_{27} – C_{29} regular steranes (with 1σ less than the width of the triangular points) from section B (upright

triangles) and C (inverted triangles). The extinction probability of individual horizons was calculated (by dividing numbers of extinction species by the total number of species excluding originating species) from previously reported high-resolution species-occurrence records⁸. Mass extinctions ME1, 2 and 3 show the start horizons of the three previously proposed extinction events^{12,27}. ME1 is associated with the loss of the latest Permian reef ecosystem in South China, which corresponds to bed 24e at Meishan. ME2 is the disappearance of most benthos at beds 25–26, and ME3 is the disappearance of the final Permian brachiopods at beds 28–29. Numerical data can be found in Supplementary Tables 1 and 2.

letters to nature

($r^2 = 0.04$) between T_{\max} values and 2-MHP indices through the section (Fig. 2). Moreover, facies changes cannot explain the observed variation; although proposed water-column deepening at beds 24e, 25 and 28 (refs. 11–13) do coincide with 2-MHP minima, the maxima in 2-MHP indices are not associated with lithological or facies variation. In fact, 2-MHP indices show no significant correlation with total organic carbon (TOC) content ($r^2 = 0.06$), and vary within individual beds (for example, beds 26 and 29; Fig. 2). Thus, the observed changes in 2-MHP indices probably reflect changes in the bacterial community structure. Because the 2-MHP index is a ratio, changes in values could reflect either changes in cyanobacterial (2-MHP) or total bacterial (HP) abundances. However, TOC-normalized abundances of 2-MHP and the ratio of 2-MHP to steranes (biomarkers of eukaryotes, primarily algae) have maxima coincident with those of the 2-MHP indices (Fig. 1), indicating that changes in the cyanobacterial populations underlie the observed trends.

In order to understand the relationship between microbial change and faunal variation, we counted the numbers of faunal species becoming extinct, together with the survivors and originating species at each horizon across the P/Tr boundary of the Meishan sections (Fig. 1 and Supplementary Table 2). This allowed calculation of extinction probability (by dividing the numbers of extinction species by the total numbers of species, excluding the originating species, at a given level) for each stratigraphic horizon⁸.

The record revealed two pulses of faunal extinction at beds 25 and 28–29 (Fig. 1 and Supplementary Table 2). It is likely that these correspond, respectively, to the previously proposed mass extinctions 2 and 3 documented in several sections in southern China¹². This correlation between the reported multiple mass extinctions and specific horizons at the Meishan sections has previously been inferred⁸. Critically, the extinction probability and the 2-MHP indices are stratigraphically coupled, with minima in 2-MHP indices coinciding with, or slightly preceding, the times of maximum extinction, while maxima in 2-MHP indices clearly lag extinction.

Based on the above, it appears that faunal and microbial turnover were closely related. This probably reflects: (i) distinct but coincidental responses to external environmental forcings, for example, nutrient fluctuations; (ii) changes in both microbial and faunal populations, reflecting their ecological coupling (for example, grazing pressure or space competition); or (iii) a combination of the two. Moreover, the change in planktonic cyanobacterial populations at Meishan appears to coincide with the expansion of cyanobacterial benthos in a vast area of the eastern Tethys and Panthalassa inferred from petrological investigation of microbialites¹. These authors proposed that benthic invertebrates limited benthic cyanobacterial populations by co-opting space and grazing, such that extinction of benthic invertebrates allowed the cyanobacteria to expand¹². However, the former mechanism probably does not apply to the Meishan sections because photosynthetic microbial mats are not expected in the shelf margin to deeper-water slope facies (above bed 24e; refs 8, 14). Given this, the Meishan 2-MHP indices probably record changes in the planktonic community, reflecting changes in nutrient status¹⁵ or grazing pressures¹⁶.

The size of phytoplankton populations, including cyanobacterial members, can be suppressed by grazing^{15–17}. Significantly, grazing pressure in the wake of the P/Tr extinction could have been much reduced in the photic zone, causing the expansion of cyanobacterial populations. The end-Permian faunal extinctions have apparently selected for planktotrophs^{16,18}, which are dominant in warm, shallow, low-latitude waters and feed on phytoplankton¹⁸; this has previously been invoked as a mechanism for photoautotroph population expansions at the P/Tr boundary^{15,19}. The association of enhanced 2-MHP abundances relative to steranes with the two episodes of faunal mass extinction (Fig. 1 and Supplementary Table 1) suggests that reduced grazing might specifically favour cyanobacterial expansion relative to planktonic algae.

The temporal lags in geological magnitude between faunal extinction and maximum cyanobacterial expansion are longer than the delays in population changes between predator and prey in modern ecosystems²⁰. However, previous workers have shown that trophic relationships, including those between phyto- and zooplankton, can develop over extended time periods in the wake of an extinction event²¹. For example, a lag between microzooplankton and microphytoplankton diversity changes, linked through trophic relationships, was recently identified in Middle Ordovician strata²²; likewise, a proliferation of acritarchs occurs 1–2 m above the P/Tr faunal mass extinction in strata from Tesero, Italy²³. Our P/Tr record is also similar to the photoautotroph response to the Cretaceous/Tertiary (K/T) extinction event, which apparently resulted in temporarily low marine productivity followed by enhanced productivity a few hundred thousand years later²¹.

Although a decrease in grazing pressure is a likely explanation for the cyanobacterial expansion observed here, a contribution from changes in nutrient dynamics cannot be excluded. Cyanobacterial proliferation has been observed in response to enhanced nutrient inputs in modern aquatic environments²⁴. Elevated nutrient levels in the end-Permian seas and oceans could have been caused by intense weathering throughout Pangea, as documented by end-

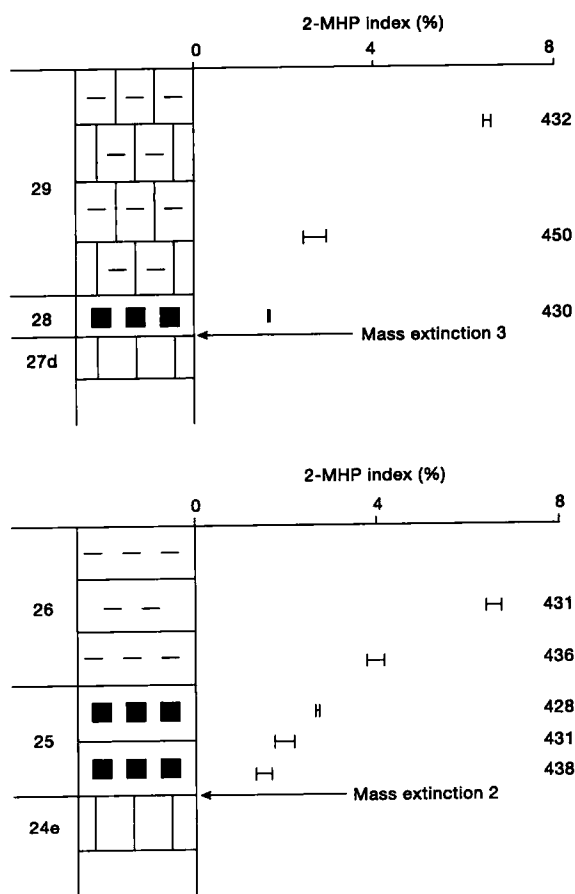


Figure 2 Plots showing the increase in 2-MHP indices (error bars, 2σ) within individual beds after the faunal mass extinctions 2 and 3, together with the T_{\max} values (numbers on right-hand side) indicating the maturity of the organic matter. Numerical data can be found in Supplementary Tables 1 and 2.

Permian pedoliths²⁵ and changed geomorphology as a result of rooted vegetation loss²⁶.

Regardless of the detailed mechanisms, the striking aspect of the Meishan 2-MHP profile is the presence of two distinct maxima within the investigated intervals. The pattern and cause of the marine mass extinction near the P/Tr boundary are still debated^{8,12,27,28}, in part because only faunal (and a small amount of calcareous algae) records of biotic change have been developed. A stepwise, multi-phase biotic extinction proposed by others on the basis of several southern China sections^{12,27}, has recently been challenged by a proposal of a main, sudden biotic crisis at beds 25–26 (ref. 28). However, the change in the 2-MHP index we report is equally dramatic (from minima to maxima) at both beds 25–26 and 28–29, such that a two-phase biotic crisis is supported not only by faunal extinctions, the interpretation of which has been the subject of debate, but also by substantial changes in the microbial community. The large changes in cyanobacterial population abundances revealed by the 2-MHP record, coupled with faunal mass extinction, probably indicate a stepwise and major environmental perturbation. Our study provides a window into the ecological restructuring, possibly at the base of the food chain, that occurred during this major faunal mass extinction. □

Methods

The solvents (HPLC grade) used were distilled twice. Tools used to prepare rock samples were rinsed with methanol and dichloromethane. Glassware was cleaned with detergent (Micro), rinsed with distilled water and annealed at 450 °C for 12 h. Aluminium foils were combusted at 450 °C for 12 h. Samples were processed in batches of six, including one procedural blank to monitor laboratory contamination.

The samples for lipid analysis were taken from section B and C at Meishan⁹, 0.5–1.5 m back from the exposed cliff. The air-dried samples were ground to <80 mesh and 100–300 g Soxhlet-extracted with chloroform for 72 h with native copper added to remove sulphur. The extract was concentrated on a rotary evaporator under reduced pressure and transferred to a small vial. After evaporation of the remaining solvent, the total extractable lipid was weighed. The asphaltenes in the extracts were eliminated by precipitation in petroleum ether. The saturated hydrocarbons, aromatics and non-hydrocarbons were fractionated by column chromatography (silica gel 60), using sequential elution with petroleum ether, benzene and ethanol.

The saturated hydrocarbons were then analysed by GC/MS using a Hewlett-Packard 5973A MS, interfaced directly with a 6890 GC equipped with a HP-5MS fused silica capillary column (30 m × 0.25 mm inner diameter; 0.25 µm film thickness). The operating conditions were as follows: temperature ramped from 70 to 280 °C at 3 °C min⁻¹ and held at 280 °C for 20 min with He as the carrier gas; the ionization energy of the mass spectrometer was set at 70 eV; the scan range was *m/z* 50–550. 2-MHP indices were calculated from the peak area of the compounds in mass chromatograms of *m/z* 191 (C₃₀) for αβ-hopane and *m/z* 205 (C₃₁) for its 2α-methyl analogue (similar profiles are generated if 2-MHP indices are calculated using higher molecular mass 2-MHPs and HPs). These are expressed as the 2-MHP index = (205/191) × 100. Sterane abundances used to calculate 2-MHP/sterane ratios were measured from the peak areas of the *m/z* 217 mass chromatograms. 2-MHPs were not detected in the procedural blanks using GC/MS analysis.

Received 26 August 2004; accepted 18 January 2005; doi:10.1038/nature03396.

- Lehrmann, D. J. et al. Permian-Triassic boundary sections from shallow-marine carbonate platforms of the Nanpanjiang Basin, south China: Implications for oceanic conditions associated with the end-Permian extinction and its aftermath. *Palaeogeogr. Palaeoclimatol. Palaeoecol.* **18**, 138–152 (2003).
- Sheehan, P. M. & Harris, M. T. Microbialite resurgence after the Late Ordovician extinction. *Nature* **430**, 75–78 (2004).
- Knoll, A. H. & Walter, M. W. Latest Proterozoic stratigraphy and Earth history. *Nature* **356**, 673–678 (1992).
- Summons, R. E., Jahnke, L. L., Hope, J. M. & Logan, G. A. 2-Methylhopanoids as biomarkers for cyanobacterial oxygenic photosynthesis. *Nature* **400**, 554–557 (1999).
- Simonin, P., Jurgens, U. J. & Rohmer, M. Bacterial triterpenoids of the hopane series from the prochlorophyte *Prochlorothrix hollandica* and their intracellular localization. *Eur. J. Biochem.* **241**, 865–871 (1996).
- Rohmer, M., Bouvier-Nave, P. & Ourisson, G. Distribution of hopanoid triterpenes in prokaryotes. *J. Gen. Microbiol.* **130**, 1137–1150 (1984).
- Rohmer, M., Bissleret, P. & Neunlist, S. in *Biological Markers in Sediments and Petroleum* (eds Moldovan, J. M., Albrecht, P. & Philp, R. P.) 1–17 (Prentice Hall, New Jersey, 1992).
- Jin, Y. G. et al. Pattern of marine mass extinction near the Permian-Triassic boundary in South China. *Science* **289**, 432–436 (2000).
- Yin, H., Zhang, K., Tong, J., Yang, Z. & Wu, S. The Global Stratotype Section and Point (GSSP) of the Permian-Triassic boundary. *Episodes* **24**, 102–114 (2001).
- Brocks, J. J., Buick, R., Summons, R. E. & Logan, G. A. A reconstruction of Archean biological diversity based on molecular fossils from the 2.78 to 2.45 billion-year-old Mount Bruce Supergroup, Hamersley Basin, Western Australia. *Geochim. Cosmochim. Acta* **67**, 4321–4335 (2003).
- Wignall, P. B. & Hallam, A. Griesbachian (Earliest Triassic) palaeoenvironmental changes in the Salt

- Range, Pakistan and Southeast China and their bearing on the Permian-Triassic mass extinction. *Palaeogeogr. Palaeoclimatol. Palaeoecol.* **102**, 215–237 (1993).
- Yin, H. et al. The Palaeozoic-Mesozoic Boundary, Candidates of Global Stratotype Section and Point of the Permian-Triassic Boundary (China Univ. of Geosciences Press, Wuhan, 1996).
- Lai, X., Wignall, P. & Zhang, K. Palaeoecology of the conodonts *Hindeodus* and *Clarkina* during the Permian-Triassic transitional period. *Palaeogeogr. Palaeoclimatol. Palaeoecol.* **171**, 63–72 (2001).
- Yin, H. & Tong, J. Multidisciplinary high-resolution correlation of the Permian-Triassic boundary. *Palaeogeogr. Palaeoclimatol. Palaeoecol.* **143**, 199–212 (1998).
- Hallam, A. & Wignall, P. *Mass Extinctions and their Aftermath* (Oxford Univ. Press, Oxford, 1997).
- Valentine, J. W. & Jablonski, D. Mass extinctions: sensitivity of marine larval types. *Proc. Natl Acad. Sci. USA* **83**, 6912–6914 (1986).
- Dionisio-Pires, L. M., Jonker, R. R., Van Donk, E. & Laanbroek, H. J. Selective grazing by adults and larvae of the zebra mussel (*Dreissena polymorpha*): application of flow cytometry to natural seston. *Freshwat. Biol.* **49**, 116–126 (2004).
- Erwin, D. H. The end-Permian mass extinction. *Annu. Rev. Ecol. Syst.* **21**, 495–516 (1990).
- Racki, G. Silica-secreting biota and mass extinctions: survival patterns and processes. *Palaeogeogr. Palaeoclimatol. Palaeoecol.* **154**, 107–132 (1999).
- Keeling, M. J., Wilson, H. B. & Pacala, S. W. Reinterpreting space, time lags, and functional responses in ecological models. *Science* **290**, 1758–1761 (2000).
- Erwin, D. H. Lessons from the past: biotic recoveries from mass extinction. *Proc. Natl Acad. Sci. USA* **98**, 5399–5403 (2001).
- Vecoli, M. & Le Herisse, A. Biostratigraphy, taxonomic diversity and patterns of morphological evolution of Ordovician acritarchs (organic-walled microphytoplankton) from the northern Gondwana margin in relation to palaeoclimatic and palaeogeographic changes. *Earth-Sci. Rev.* **67**, 267–311 (2004).
- Rampino, M. R. & Adler, A. C. Evidence for abrupt latest Permian mass extinction of foraminifera: results of tests for the Signor-Lipps effect. *Geology* **26**, 415–418 (1998).
- Mastin, B. J., Rodger, J. H. Jr & Deardorff, T. L. Risk evaluation of cyanobacteria-dominated algal blooms in a North Louisiana reservoir. *J. Aquatic Ecosyst. Stress Recovery* **9**, 103–114 (2002).
- Retallack, G. J. Search for evidence of impact at the Permian-Triassic boundary in Antarctica and Australia. *Geology* **26**, 979–982 (1998).
- Ward, P. D., Montgomery, D. R. & Smith, R. Altered river morphology in South Africa related to the Permian-Triassic extinction. *Science* **289**, 1740–1743 (2000).
- Yang, Z. Y. et al. *Permian-Triassic Events of South China* (Geological Publishing House, Beijing, 1993).
- Erwin, D. H., Bowring, S. A. & Jin, Y. in *Special Paper 356, Catastrophic Events and Mass Extinctions: Impacts and Beyond* (eds Koeberl, C. & MacLeod, K. G.) 363–383 (Geological Society of America, Boulder, 2002).

Supplementary Information accompanies the paper on www.nature.com/nature.

Acknowledgements We thank F. Yang, S. Wu, G. Zhu, J. Huang, Y. Yi and J. Yu for field assistance, L. Lu, D. Jiao and X. Huang for sample processing, and M. Benton for constructive comments on the manuscript. The authors thank I. D. Bull and R. Berstan for their technical assistance and the NERC for funding the Bristol node of the Life Sciences Mass Spectrometry Facility (<http://www.chm.bris.ac.uk/lsmf/index.html>). This work was supported by National Natural Science Foundation (H. Y.), NCET programme of Ministry of Education of China (S. X.) and the Lab of Bio- and Environmental Geology in China University of Geosciences.

Competing interests statement The authors declare that they have no competing financial interests.

Correspondence and requests for materials should be addressed to R.D.P. (r.d.pancost@bristol.ac.uk).

Affinities of 'hyopsodontids' to elephant shrews and a Holarctic origin of Afrotheria

Shawn P. Zack¹, Tonya A. Penkrot¹, Jonathan I. Bloch² & Kenneth D. Rose¹

¹Center for Functional Anatomy and Evolution, The Johns Hopkins University School of Medicine, 1830 East Monument Street, Baltimore, Maryland 21205, USA

²Florida Museum of Natural History, University of Florida, Gainesville, Florida 32611-7800, USA

Macroscelideans (elephant shrews or sengis) are small-bodied (25–540 g), cursorial (running) and saltatorial (jumping), insectivorous and omnivorous¹ placental mammals represented by at least 15 extant African species classified in four genera². Macroscelidea is one of several morphologically diverse but predominantly African placental orders classified in the superorder

Suppression of interferences for direct determination of arsenic in geological samples by inductively coupled plasma mass spectrometry

Zhaochu Hu,^{*ab} Shan Gao,^{ab} Shenghong Hu,^b Honglin Yuan,^a Xiaoming Liu^a and Yongsheng Liu^b

^a Key Laboratory of Continental Dynamics, Department of Geology, Northwest University, Xi'an, 710069, PR China. E-mail: zchu@vip.sina.com; Fax: +86 29 88303447; Tel: +86 29 88302905

^b State Key Laboratory of Geoprocesses and Mineral Resources, China University of Geosciences, Wuhan, 430074, PR China

Received 20th May 2005, Accepted 19th July 2005

First published as an Advance Article on the web 23rd August 2005

We have developed a method for direct determination of arsenic in geological samples using ICP-MS by reduction of interferences, without preconcentration, separation and use of the hydride generation technique. Concentrations of HNO₃ have a significant effect on the arsenic signal. This type of interference cannot be corrected by internal standards (Rh and In) because the signal suppression due to HNO₃ is apparently dependent on the first ionization potential of elements. Addition of 4% (v/v) ethanol to 1–10% (v/v) HNO₃ was found to be an excellent method for reducing this type of matrix effect from 30–40% to less than 5% for high first ionization potential elements ⁷⁵As (9.81 eV), ⁸²Se (9.75 eV), and ¹²⁶Te (9.01 eV). Direct determination of arsenic in geological samples by ICP-MS is often complicated by the presence of Nd²⁺, Sm²⁺ and Eu²⁺ interferences, in addition to the well known interference of ArCl⁺, and the high first ionization potential of As (9.81 eV) also results in relatively low analytical sensitivity in ICP-MS. It is shown that both problems can be overcome by a combination of a 4% ethanol matrix modifier with nebulizer gas flow rate adjustment. For example, the interference from doubly charged ions of a rare earth element (Ce²⁺) is reduced by a factor of 30 with the addition of 4% ethanol at a nebulizer gas flow rate of 1.00 l min⁻¹ and rf power of 1350 W, while the signal intensity of As is similar in both solutions. A nebulizer gas flow rate of 0.94 l min⁻¹, an rf power of 1350 W and 4% ethanol modifier were chosen in practical sample analysis. Under these conditions, the interference of doubly charged ions of the rare earth element (Ce²⁺) was reduced by a factor of 6.5 and the signal intensity of As was improved by a factor of 3 relative to that in 3% (v/v) HNO₃ solution at the corresponding optimum nebulizer gas flow rate of 0.98 l min⁻¹ and rf power of 1350 W. The arsenic equivalent concentration caused by ArCl⁺ interference was reduced by a factor of 10 under our given experimental conditions in the presence of 4% (v/v) ethanol. The developed method was applied to the direct determination of arsenic in a series of international geological reference materials. Most of the results were found to be in reasonable agreement with the reported values in the literature, particularly for those having recommended values. This simple method shows a great potential for the direct determination of arsenic in geological and environmental samples.

Introduction

Although ICP-MS has been widely applied for the direct determination of multi-elements in geological samples,^{1–3} very few publications have been devoted to the direct determination of arsenic in geological samples by ICP-MS. As with many other spectrometric techniques, ICP-MS is subject to both spectral and non-spectral interferences. In most cases, spectral interferences can be avoided by choosing alternative isotopes, since most elements in the Periodic Table have several isotopes. This method, however, cannot be applied to the analysis of mono-isotopic elements like As (74.92 amu). In atomic spectroscopy, the hydride generation technique has been routinely coupled for the determination of As, because spectral interferences are minimized and detection limits are improved by this approach.^{4–14} However, the generation of AsH₃ is normally carried out in the presence of a high concentration of HCl, which may interfere with the determination of As by ICP-MS because of the formation of ArCl⁺. HNO₃ has been used to avoid the ArCl⁺ interference.⁹ Unfortunately, HNO₃ oxidizes As(III) to As(V),

leading to a lower efficiency of the hydride generation process.^{10,11} Special membrane separators are needed to minimize the transportation of chloride to the plasma.¹² Owing to the complicated matrix composition of geological samples, separation of As from the well documented liquid phase interferences (e.g., Cu, Ni, Co) is also required before undertaking HG measurements. This has been done routinely by addition of masking agents^{10,11} or co-precipitation with La(OH)₃.^{7,13} High blank levels, long memory effects and plasma instability are other problems in HG measurement.^{8,14} High resolution magnetic sector field ICP-MS can be used to separate Nd²⁺, Eu²⁺, Sm²⁺ and ArCl⁺ interferences from arsenic (a resolution of $M/\Delta M = 8000$ is required). Although the overall sensitivity of magnetic sector ICP-MS in the low-resolution mode of $M/\Delta M = 300$ is at least 10 times higher than for quadrupole instruments, the sensitivity at $M/\Delta M = 7800$ yields an intensity of only 0.5–2% compared with $M/\Delta M = 300$.¹⁵ Electrothermal vaporization is another possibility,^{16,17} but the complexity of the procedure may have prevented the method from being widely used.

DOI: 10.1039/b507200j

The upper, middle and lower crust abundances of arsenic are estimated to be 4.8, 2.4 and 0.2 $\mu\text{g g}^{-1}$, respectively,¹⁸ which suggest that the As content in most geological samples should be high enough to be directly determined by ICP-MS. However, the direct determination of arsenic in geological samples by ICP-MS is hampered by interferences from Nd^{2+} , Sm^{2+} and Eu^{2+} in addition to the well known interference of ArCl^+ . Precise results are difficult to obtain, especially for those samples with high rare earth elements and Cl content and lower arsenic concentration.¹⁹ It has been well documented that the addition of organic solvent can significantly improve the sensitivity of As^+ and suppress the interference of ArCl^+ in ICP-MS.^{20–29} We have entered into detailed discussion about the volatile organic solvent induced signal enhancement effects in ICP-MS.²⁹ The introduction of organic solvent into ICP-MS may produce carbon deposits on the interface, ionic lenses and torch and fluctuation of the plasma due to the high energy necessary to dissociate organic molecules.²⁸ In this study we adopt a microconcentric nebulizer, which greatly reduces the organic solvent load on the plasma, with the consequence of negligible carbon deposits on the sampling cone after one-hour of continuous aspiration of 4% (v/v) ethanol.

The closed, pressurized digestion system has been widely used to decompose geological samples for multi-element determinations such as rare earth elements and high field strength elements.^{30,31} Digestions performed in such devices benefit from synergic effects of temperature and pressure. This technique is generally much more efficient than conventional wet digestions in open systems: the loss of volatile elements is prevented, the use of reagent is reduced and the decomposition of insoluble minerals is more efficient. For studies involving the analysis of a large number of samples (e.g., estimation of crustal compositions, geochemical exploration and soil composition surveys), it was clear that time-consuming sample preparation techniques like on- or off-line matrix separation methods are not suitable.^{32,33} As many elements as possible need to be determined in a single sample solution for reasons of low analytical cost and high sample throughput. In this study, the closed, pressurized digestion method used for multi-elements determinations is tested for the determination of arsenic.

Our objective in this study is to develop a simple, precise method for the direct determination of As in geological samples by quadrupole ICP-MS. Research was focused on the reduction of doubly charged ions and ArCl^+ interferences, and the improvement of arsenic signal intensity by the addition of ethanol or Triton X-100 solution. The reductions of nitric acid concentration on the responses of high first ionization potential elements (As, Se, Te and Sb) and internal standards (In and Rh) were also investigated. The developed method was validated by analyzing a series of international rock standard reference materials.

Experimental

Instrumentation

A PerkinElmer SCIEX ELAN 6100DRC (dynamic reaction cell) ICP-MS instrument was used with the outer and intermediate ICP gas flow rates fixed at 13.2 and 1.2 l min^{-1} , respectively. A glass microconcentric nebulizer (MCN) and a cyclonic spray chamber comprised the sample introduction system. The typical sample uptake rate was 0.20 ml min^{-1} by self uptake. The nebulizer gas flow rate and rf power were variable and will be described where appropriate. The auto lens voltages were set by optimizing a solution of 10 ng ml^{-1} Mg, Co, As, Rh, Ce, Pb and U. For data acquisition, peak hopping was used with a dwell time of 1 s. There were three sweeps per reading and one reading per replicate.

Reagents

All reagents used were of analytical grade. Ultra-pure water with a resistivity of 18.0 $\text{M}\Omega \text{ cm}^{-1}$ was obtained from a Milli-Q water purification system (Millipore, USA). Ultra-pure nitric acids were prepared by sub-boiling distillation in a commercially available quartz still, while hydrofluoric acid and ethanol were doubly distilled in a home-made sub-boiling distillation device. Hydrofluoric acid was found to contain a high As content (about 200 ng ml^{-1}), which made precise analysis impossible. The conventional sub-boiling purification procedure is not effective in the reduction of As impurity in HF. This could be related to the presence of volatile As species like AsF_3 (boiling point 63 °C). To remove this volatile As species, a boiling procedure for hydrofluoric acid was adopted before using the conventional sub-boiling purification procedure. The concentration of As in our finally used hydrofluoric acid was about 1 ng ml^{-1} . Multi-element mixed stock solution was prepared from 1.0 mg ml^{-1} of single element standard solutions (National Center for Analysis and Testing of Steel Materials, China). Unless otherwise indicated, all the ethanol and Triton X-100 solutions mentioned below contain 3% (v/v) HNO_3 .

Geological reference samples

To investigate the accuracy and precision of the proposed method, a series of international geological reference materials were analyzed. These rocks cover the whole compositional spectrum of igneous rock, ranging from ultramafic (peridotite JP-1; dunite DTS-1) to mafic (basalts GSR-3, JB-3, BHVO-1, BIR-1; dolerite DNC-1; diabase W-2) to intermediate (andesites GSR-2, JA-3, AGV-1; granodiorite JG-3) and finally to acidic (granites GSR-1, G-2; rhyolite RGM-1). They also include the most common sedimentary rocks of sandstone (GSR-4), shale (GSR-5) and limestone (GSR-6).

Sample decomposition procedure

Fifty milligrams of sample powder of less than 200 mesh were placed in a home-made PTFE-lined stainless steel bomb to which were added 1.00 ml of HNO_3 and 1.00 ml of HF. The sealed bomb was then placed in an electric oven and heated to 190 °C for 48 h. After cooling, the bomb was opened and placed on a hot plate (at 120 °C), and evaporated to incipient dryness on the hot-plate (but not baked). 1.00 ml of HNO_3 was added, evaporated to dryness and followed by a second addition of HNO_3 and evaporation to dryness. The residue was then dissolved by adding 1.50 ml of HNO_3 and 2.50 ml of ultra-pure water. Next the bomb was capped and left on the hot-plate overnight. The final solution was made up to 50 ml by addition of ultra-pure water and 0.50 ml of 1 mg l^{-1} Rh internal standard solution. This sample decomposition method has been routinely used for analysis of multi-elements in geological samples in our laboratory. For the As determination, 4.80 ml each of these solutions were taken and 0.20 ml of ethanol solvent added. A reagent blank solution was prepared in the same way.

Results and discussion

Suppression of the nitric acid matrix effect

In inductively coupled plasma optical emission spectrometry (ICP-OES), acid matrix effects are known to cause signal suppression with increased acid concentrations.³⁴ A comparison of acid matrix effects by Pickford and Brown³⁵ indicated that they are more severe in ICP-MS than in ICP-OES. There are many methods to compensate for acid matrix effects, such as matrix matching,³⁶ internal standardization,³⁷ isotope dilution³⁸ and standard addition.³⁹ However, few studies have